Atlas of the Embryonic Brain in the Pygmy Squid, Idiosepius paradoxus

Authors: Yamamoto, Masamichi, Shimazaki, Yumiko, and Shigeno, Shuichi

Source: Zoological Science, 20(2) : 163-179

Published By: Zoological Society of Japan

URL: https://doi.org/10.2108/zsj.20.163

ZOOLOGICAL SCIENCE **20**: 163–179 (2003)

Atlas of the Embryonic Brain in the Pygmy Squid, *Idiosepius paradoxus*

Masamichi Yamamoto[1], Yumiko Shimazaki[1] and Shuichi Shigeno[2*]

[1]*Ushimado Marine Laboratory, Okayama University, Ushimado, Okayama 701-4303, Japan*
[2]*Evolutionary Regeneration Group, RIKEN Center for Developmental Biology, Kobe, Hyogo 650-0047, Japan*

ABSTRACT—Gross structural changes and neuropil formation in the brain during development were described in *Idiosepius paradoxus*, a sepioid that we chose as a model cephalopod. The brain originates in 4 pairs of ectodermal placodes, which occur separately in the embryonic surface undergoing epiboly. In the final period of epiboly, neuroblasts internalize from the placodes and gather into 4 pairs of ganglionic masses. The ganglionic masses assemble into a ring-like cluster encircling the inner yolk and the foregut anlage, gradually integrated into the 4 domains of a massive brain, a subesophageal mass (SBM), a supraesophageal mass (SPM), and a pair of optic lobes. In the early brain, neuropil forms a framework composed of a longitudinal ladder lying in the SBM, and a transverse arch standing on the lateral sides of the SBM and crossing the SPM. Differentiation of brain lobes proceeds from ventral to dorsal along this framework; first the magnocellular lobes and the posterior pedal lobe appear first in the SBM, the other lobes in the SBM and the basal lobes follow in the proximal region of the SPM, and the accessory lobes develop last in the most dorsal zone of the SPM. In the hatchlings, the brain lobes show almost the same arrangement as in the adults, but the accessory lobes, particularly the vertical lobe, are much smaller than those in the adults. Comparison of the present results with those in the teuthoid and the octopod indicates that developmental sequences of the brain are highly conserved in the coleoid cephalopods.

Key words: cephalopods, embryonic development, central nervous system, brain lobe, neuropil

INTRODUCTION

The highly developed nervous systems of the cephalopod have been important materials for neurocytology, electrophysiology and biophysics (for reviews see Gilbert *et al*., 1990; Abbott, 1995). The anatomical structures of cephalopod central nervous systems have extensively been examined by Young (1965, 1971, 1974, 1976, 1977, 1979) and Messenger (1979).

Ontogeny of the cephalopod is characterized by a unique discoidal cleavage and a direct mode of development devoid of a typical larval form. The brain anlagen occur in the embryonic surface with primordia of other ectodermal organs, and assemble into a massive embryonic brain, which directly develops into the adult brain. Since the classical studies by Kölliker (1844) and Korschelt (1892), development of the cephalopod brain had long been ignored until Meister (1972) and Marquis (1989) published histological works in *Loligo vulgaris* and *Octopus vulgaris*, respectively. We undertook comprehensive studies of brain development in the cephalopod. Since basic information was lacking on the embryonic brain of the cephalopod, we started our work from morphological description using conventional histological techniques. We have already described the basic processes of brain development in two teuthoid squids, *Sepioteuthis lessoniana* (loliginid) (Shigeno *et al*., 2001d) and *Todarodes pacificus* (ommastrephid) (Shigeno *et al*., 2001b, c). The developmental sequences of the brain in the teuthoids were very similar to that in an octopod, *O. vulgaris* (Marquis, 1989).

Since eggs of *S. lessoniana* and *T. pacificus* were difficult to obtain in the above studies, we considered it essential to find a model cephalopod species suitable for developmental studies. After an extensive survey, we chose a pygmy squid *Idiosepius paradoxus* (sepioid) as a model species because of the following advantages: (1) This species is widely distributed in littoral waters along the coast of Japan (Sasaki, 1929), and many individuals are easily collectable with a hand net in the eelgrass beds. (2) The adults, ca. 1.5cm in mantle length, can be maintained in the small

* Corresponding author: Tel. +81-78-306-3084;
FAX. +81-78-306-3083.
E-mail: shigeno@cdb.riken.go.jp

vessel in the laboratory. (3) The fertilized eggs are constantly obtainable throughout the year in the laboratory. One female lays 30-80 eggs repeatedly for more than one month. The embryos develop at a considerably rapid rate in a shallow glass dish (Yamamoto, 1988). (4) Transparency and a small size (ca. 1 mm in major axis) of the egg make it possible to apply various cytological techniques to live or whole mount specimens.

The purposes of the present study are: (1) to provide a basic atlas of the embryonic brains for future developmental studies in *I. paradoxus,* and (2) to compare the developmental pattern of the brain in the sepioid with those in the teuthoid (Meister, 1972; Shigeno et al, 2001b-d) and the octopod (Marquis, 1989). Before the present study, we examined the organization of the nervous system in the adult *I. paradoxus* (Shigeno and Yamamoto, 2002). In that study, we confirmed that configuration of the brain lobes is generally similar to that described in *Loligo* by Young (1974, 1976, 1977, 1979) and Messenger (1979).

MATERIALS AND METHODS

Animals

Adults of *Idiosepius paradoxus* (Ortmann, 1881) (Sepiida, Idiosepiidae) were caught with a coarse tow net from April through July in the eelgrass beds near the Ushimado Marine Laboratory, which is located on the coast of the Seto Inland Sea of Japan. Mature females were maintained in an outdoor aquarium supplied with running seawater under the natural light cycles, and fed with small shrimps and amphipods collected in the eelgrass beds. To obtain fertilized eggs, green plastic strips, 5 mm in width, were floated in the aquarium. The eggs laid on the strips were allowed to develop in running sea water at 20–25°C. The embryos hatched 13 days after oviposition at 25°C. Embryonic stages were determined following the normal table by Yamamoto (1988).

Dechorionation

Mechanical removal of the chorion is difficult in the embryos before reaching stage 23 due to the narrow perivitelline space. To soften the chorion, the early embryos were immersed in 1% mercaptoacetic acid/sea water adjusted to pH 8.5 with 0.1N NaOH just before use. As soon as the chorion became soft (in 2–4 min), the embryos were transferred to normal seawater and the chorion was removed with forceps. In the embryos at and after stage 23, the chorion was directly removable with forceps.

Histology

The dechorionated embryos and hatchlings were fixed for 2 hr in 2.5% glutaraldehyde dissolved in a sucrose containing buffer solution (0.4M sucrose and 0.1M Na cacodylate, pH 7.4), and post-fixed for 1hr with 1% OsO_4 dissolved in a mixture of 1% K-ferrocyanide, 0.4M NaCl and 0.1M Na cacodylate (pH 7.4). The specimens were dehydrated through a graded ethanol series and embedded in Spurr's resin. Serial sections about 3 μm in thickness were cut with a diamond knife and stained with 1% toluidine blue (TB). Hatchlings and adults were also fixed with 4% paraformaldehyde, dehydrated in ethanol, embedded in Paraplast, and stained by Cajal's silver impregnation method modified for cephalopod specimens by Stephens (1971). The light micrographic images of histological sections were captured with a digital camera (Nikon COOLPIX 995) and were processed using Adobe Photoshop 6.0 (Adobe Systems). The cross sectional profiles in Figs. 4–8 are tracings of the captured images. The longitudinal profiles in Figs. 4–8 are drawings reconstructed from serial images.

Terminology

The terms used in the present study are based on the defini-

Table 1. Brain lobes described in the present paper

Name	abbreviation
OPTIC LOBE	OL
SUBESOPHAGEAL MASS	SBM
Anterior Subesophageal Mass	ASM
prebrachial lobe	pbrL
brachial lobe	brL
Middle Subesophageal Mass	MSM
anterior chromatophore lobe	acL
anterior pedal lobe	apL
posterior pedal lobe	ppL
ventral magnocellular lobe	vmL
Posterior Subesophageal Mass	PSM
dorsal magnocellular lobe	dmL
posterior magnocellular lobe	pmL
palliovisceral lobe	pvL
visceral lobe	vsL
fin lobe	fL
posterior chromatophore lobe	pcL
SUPRAESOPHAGEAL MASS	SPM
subpedunclulate lobe	spL
precommissure lobe	prL
anterior basal lobes	abL
anteior anterior basal lobe	aabL
lateral anterior basal lobe	labL
posterior anterior basal lobe	pabL
posterior basal lobes	pbL
median basal lobe	mbL
dorsal basal lobe	dbL
lateral basal lobe	lbL
interbasal lobe	itL
accessary lobes	
inferior frontal lobe	ifL
superior frontal lobe	sfL
subvertical lobe	svL
vertical lobe	vtL
Optic Ttract Rregion	OTR
olfactory lobe	ofL
peduncle lobe	pdL
dorso-lateral lobe	dlL
Lobes outside the brain	
inferior buccal lobe	ibL
superior buccal lobe	sbL

tions given for the adult nervous system of *Loligo* by Young (1974, 1976, 1977, 1979), Messenger (1979), and Budelmann and Young (1993). For the convenience of readers, the names of the brain lobes described in the present paper and their abbreviations are arranged in Table 1. We use the term "ganglion" for the mass of neuroblasts occurring as the brain precursor according to Meister (1972) and Marquis (1989). We, however, adopt the term "palliovisceral ganglion" in stead of "visceral ganglion" (Meister, 1972; Marquis, 1989) to avoid confusion with the visceral ganglion of the gastropods, because the two structures cannot be homologous.

RESULTS

Gross morphological changes of the brain

Formation of neurogenic placodes (Figs. 1A–D and 2A)

Development of the brain starts with the occurrence of 4 pairs of neurogenic placodes in the embryonic surface. At the beginning of the embryonic development, the cleaving blastodisc forms a blastoderm at one pole of the ellipsoidal egg (future posterior end of the embryo). The blastoderm expands over the surface of the yolk syncytium towards the opposite pole of the egg (future anterior end). The thin cellular sheet covering the yolk syncytium consists of two layers, the ectoderm and the mesentoderm. When about 2/3 of the egg surface is cellulated [Stage (St) 17], the anlagen of various ectodermal organs such as the eyes, statocysts, shell gland, and mouth appear in the form of ectodermal placodes (Fig. 1A). At this stage, 4 pairs of neurogenic placodes also occur in the equatorial zone of the embryo (Figs. 1A and 2A). They are characterized by large and lightly stained neuroblasts with a large nucleus containing prominent nucleoli (Fig. 1B–D). The neurogenic placodes are the precursors of the ganglionic anlagen of the brain: the cerebral, pedal, palliovisceral and optic ganglia. The small precursors of the cerebral ganglia (cerebral placodes, cP) appear on both lateral margins of the mouth primordium in the dorsal surface of the embryo. The slender precursors of the optic ganglia (optic placodes, oP) occur along the anterior margin of the eye primordia in the dorso-lateral surface of the embryo. The precursors of the pedal ganglia (pedal placodes, pP) are also slender, appearing in the anterior region of the statocyst primordia in the ventro-lateral surface of the embryo. The precursors of the palliovisceral ganglia (palliovisceral placodes, vP) are small, occurring on the posterior margin of the statocyst primordia in the ventro-lateral surface of the embryo. In addition to the placodes of the brain anlagen, 5 pairs of placodal precursors of the intrabrachial ganglia are arranged in a row along the anterior border of the future head (Fig. 2A).

Ingression and accumulation of the neuroblasts into ganglionic masses (Figs. 1E–G and 2B)

The neurogenic placodes internalize to form ganglionic anlagen of the brain during the final period of epiboly (St 18–19). Neuroblasts increase in number in each neurogenic placode, leave inwards from the embryonic surface, migrate in a group in between the ectoderm and the mesentoderm (Fig. 1E–G), and gather into a cell mass. The neuroblasts that ingress from each optic placode form a slender mass (optic ganglion) on the posterior margin of each eye primordium (Fig. 2B). The neuroblasts that ingress from each cerebral placode (cP) migrate in a lateral direction (Fig. 1E, F) and form a small cluster (cerebral ganglion) on each side of the oral ingrowth (primordial buccal mass) (Fig. 2B). The neuroblasts that leave each pedal placode (pP) (Fig. 1E) form a belt-like mass (pedal ganglion) along the posterior margin of the swellings of the arm anlagen, and eventually join the intrabrachial ganglia included within each arm anlage (Fig. 2B). The neuroblasts that leave each palliovisceral placode (vP) (Fig. 1G) migrate dorsally along the posterior margin of the eye primordium, and form a broad mass (palliovisceral ganglion) in the posterior end of the head region (Fig. 2B). At St 19, the anlagen of the stellate ganglia become evident as a pair of small clusters of neuroblasts within the dorsal margin of the mantle anlage (Fig. 2B).

Assemblage of the ganglionic masses into a circumesophageal ring (Figs. 1H, I and 2C, D)

At St 20, the ganglionic anlagen of the brain gradually increase in volume and change in shape through proliferation and migration of neuroblasts. Neuroblasts become smaller in size and strongly stainable with toluidine blue. The pedal ganglia join the palliovisceral ganglia near the primordial statocysts (Fig. 2C). The pedal ganglia and the palliovisceral ganglia also come into contact with the anterior margin and the posterior margin of the optic ganglia, respectively (Fig. 2C). The left and right pedal ganglia extend towards the midline of the ventral surface of the embryo (Fig. 2C). The cerebral ganglia extend both in dorsal and lateral directions (Fig. 2C).

At St 21, the left and right pedal ganglia become continuous to each other through a thin cellular belt in the ventral surface of the anterior region of the head (Figs. 1H and 2D). Each optic ganglion (oG) becomes a discrete oval body on the basal wall of the primordial eye (Fig. 1H). Three non-neural structures: the paravertical bodies, anterior chamber organs (Fig. 1H), and subpedanculate tissues (Fig. 3A) appear around the eyes and the associated optic ganglia. The left and right cerebral ganglia (cG) become thick masses on both lateral sides of the forming buccal mass (Fig. 1H, I), and join each other through a narrow cellular bridge over the buccal mass (Figs. 1H and 2D). The cerebral ganglia further extend laterally, and come into contact with the ipsilateral optic ganglia (oG) and pedal ganglia (pG) (Fig. 1H). As a result, the cerebral, pedal, and optic ganglia make a large ring of neuroblasts encircling the inner yolk and the buccal mass anlage (Fig. 1H). Each palliovisceral ganglion (vG) also joins the ring at the position near the statocyst (Figs. 1I and 2D). Thus, the primary groundwork for the brain is completed in the form of a circumesophageal ring composed of the 4 pairs of ganglionic anlagen (Fig. 2D).

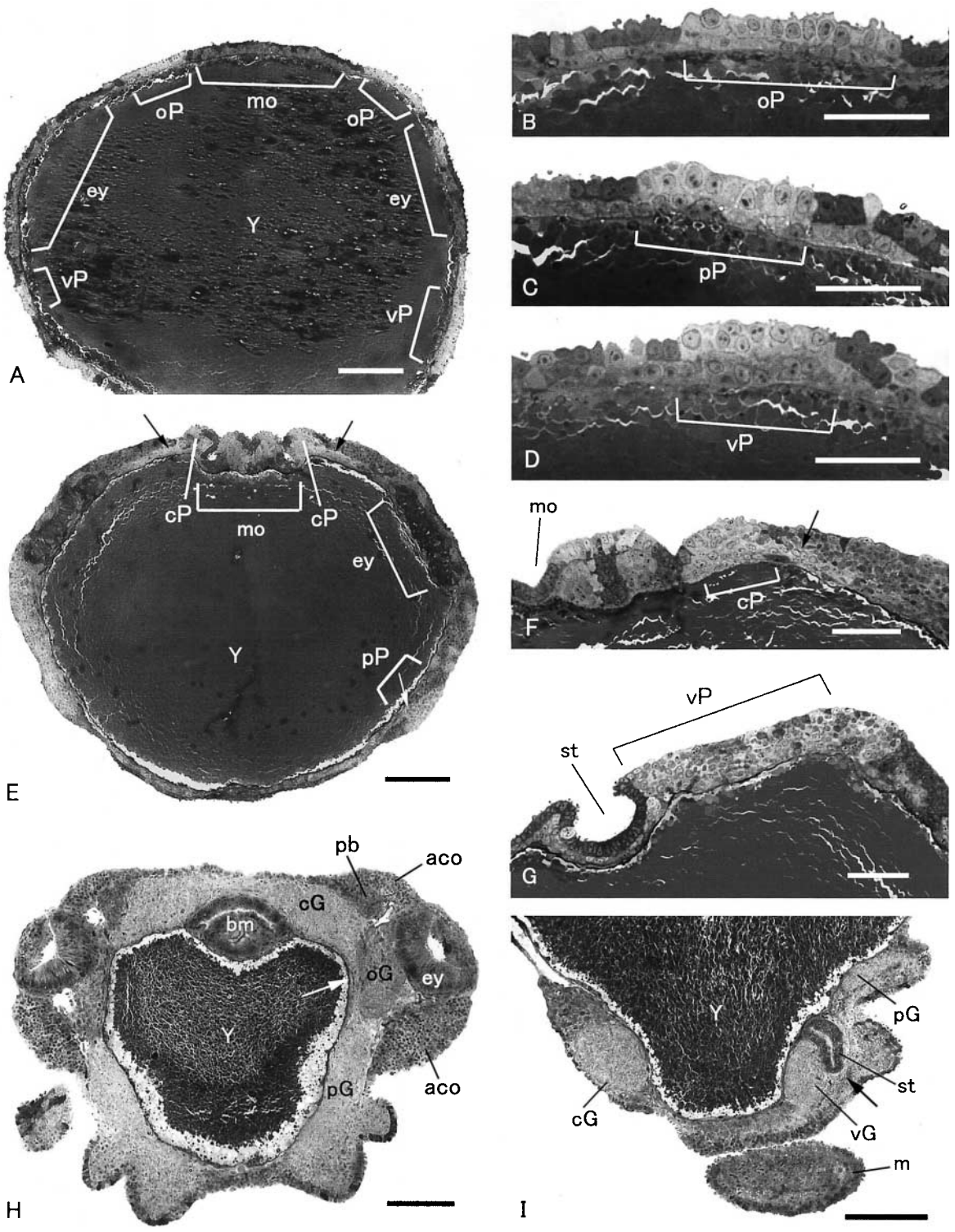

Fig. 1. Light micrographs showing the early phase of brain development. TB staining. **(A)** Transverse section of an embryo at the late stage of epiboly (St 17). The optic placodes (oP), palliovisceral placodes (vP), and the placodes of mouth (mo) and eyes (ey) are visible in the cell layer covering the yolk (Y). **(B)** An optic placode (oP) at St 17. **(C)** A pedal placode (pP) at St 17. **(D)** A palliovisceral placode (vP) at St 17. **(E)** Transverse section of an embryo at St 19. Neuroblasts are undergoing ingression from the cerebral placodes (cP) (black arrow) on both sides of the mouth anlage (mo), and from the pedal placodes (pP) (white arrow). **(F)** A cerebral placode (cP) and neuroblasts undergoing ingression (arrow) at St 19. **(G)** A palliovisceral placode (vP) near a statocyst primordium (st) at St 19. Neuroblasts are undergoing ingression and migration. **(H)** Transverse section of an embryo at St 21. The cerebral ganglia (cG), optic ganglia (oG) and pedal ganglia (pG) are continuous to each other near the base of the eye (ey) (arrow) and form a ring surrounding the yolk (Y) and the buccal mass (bm). **(I)** Para-sagittal section through a lateral side of an embryo at St 21. The arrow indicates the region where a pedal ganglion (pG) joins a palliovisceral ganglion (vG) near the statocyst (st). aco, anterior chamber organ; m, mantle; pb, paravertical body. Bar, 100 μm in **A, E, H** and **I**, and 50 μm in the others.

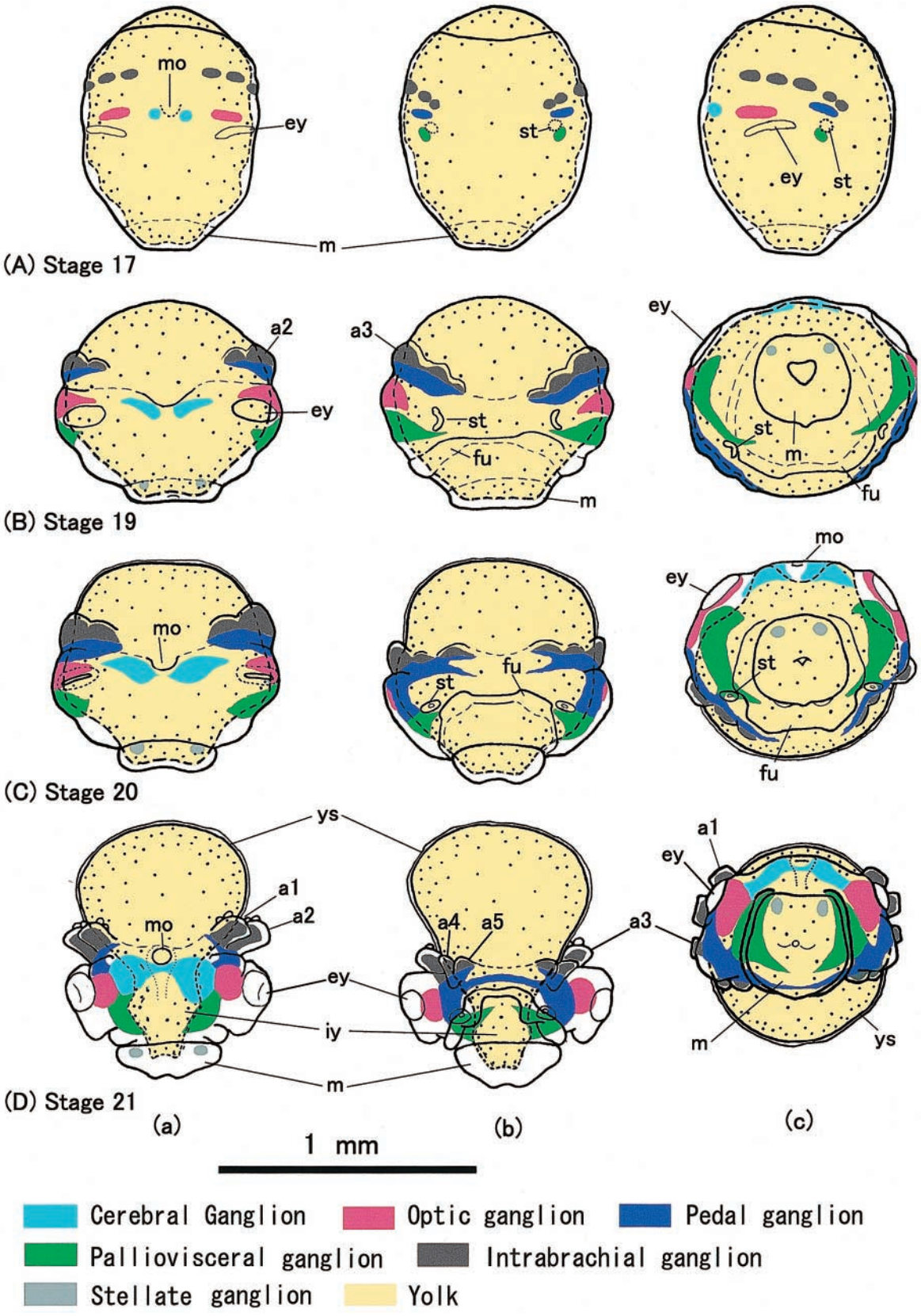

Fig. 2. Development of the brain and associated neural elements in *I. paradoxus* embryos from St 17 to 21. (**a**) Dorsal view; top, anterior. (**b**) Ventral view; top, anterior. (**c**) View from the right side (**A**), and from the posterior end (**B–D**). The brain anlagen shown in **A** are not yet ganglia but the preceding placodes. a1–5, arm1–5; ey, eye; fu, funnel; iy, internal yolk; m, mantle; mo, mouth; st, statocyst; ys; yolk sac. Bar, 1 mm.

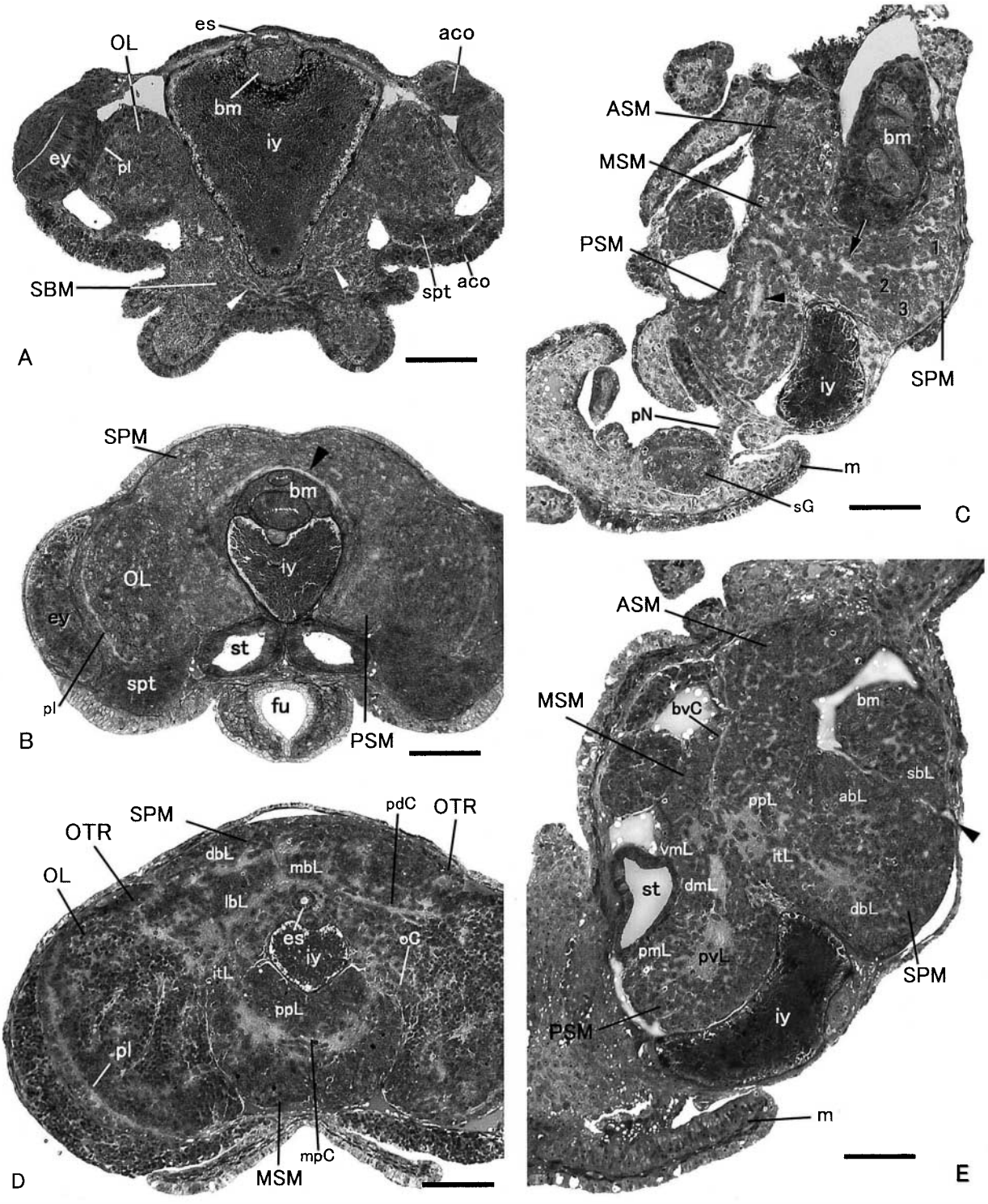

Fig. 3. Light micrographs of embryonic brains from St 22 to St 24. TB staining. (**A**) Transverse section of an embryo at St 22. The arrowhead indicates patches of neuropil occurring in the ventral area of the subesophageal mass (SBM). (**B**) Transverse section of an embryo at St 23. The arrowhead indicates a part of the transverse arch crossing the region over the dorsal surface of the buccal mass (bm). (**C**) Para-sagittal section through a lateral side of an embryo at St 23. The arrow and the arrowhead indicate a part of the longitudinal column and the transverse arch, respectively. Three branches of the transverse arch are shown by 1–3. (**D**) Transverse section of an embryo at St 24. (**E**) Para-sagittal section through a lateral side of an embryo at St 24. The arrowhead indicates a cleft between the superior buccal lobe (sbL) and the main part of the supraesophageal mass (SPM). aco, anterior chamber organ; bvC, brachial-palliovisceral connective; es, esophagus; ey, eye; fu, funnel; iy, internal yolk; m, mantle; mpC; middle pedal commissure; oC, optic commissure; pdC, peduncle commissure; pl, plexiform layer; pN, pallial nerve; sG, stellate ganglion; spt, subpedunculate tissue; st, statocyst. See Table 1 for other abbreviations. Bar, 100 μm.

Consolidation of the circumesophageal ring into a massive brain (Figs. 3–9)

The cephalopod brain is composed of 4 domains: a subesophageal mass (SBM), a supraesophageal mass (SPM), and a pair of optic lobes (OL) (Budelmann, 1995). The SBM is defined as the part derived from the pedal and the palliovisceral ganglia, and is subdivided into 3 compartments, the anterior (ASM), middle (MSM), and posterior (PSM) subesophageal masses. The pedal ganglia form the ASM and the MSM, while the palliovisceral ganglia become the PSM. The SPM is defined as the part derived from the cerebral ganglia. The optic ganglion becomes as a whole the optic lobe (OL).

At St 22, with the compaction of the embryonic body, the ring-shaped circumesophageal cluster begins transformation into a massive brain (Fig. 4A). The left and right palliovisceral ganglia join each other at the midline in the postero-ventral part of the head (Fig. 4A, B). The palliovisceral ganglia and the pedal ganglia form a continuous mass (SBM) in the ventral region of the head (Fig. 4A, B). No demarcation line is visible between the compartments derived from the palliovisceral ganglia (PSM) and the pedal ganglia (MSM and ASM), but the statocysts define the boundary between the MSM and the PSM (Fig. 4B). The boundary between the ASM and MSM is not definable at this stage. The ASM is continuous to the intrabrachial ganglia (ibG) at the anterior end (Fig. 4A, B). Each optic ganglion keeps a spherical entity and becomes optic lobe (OL) on the proximal surface of the eye (Fig. 3A). The cerebral ganglia form an arch spanning the inner yolk and the buccal mass. The arch constitutes the supraesophageal mass (SPM), which is continuous basally to the MSM and laterally

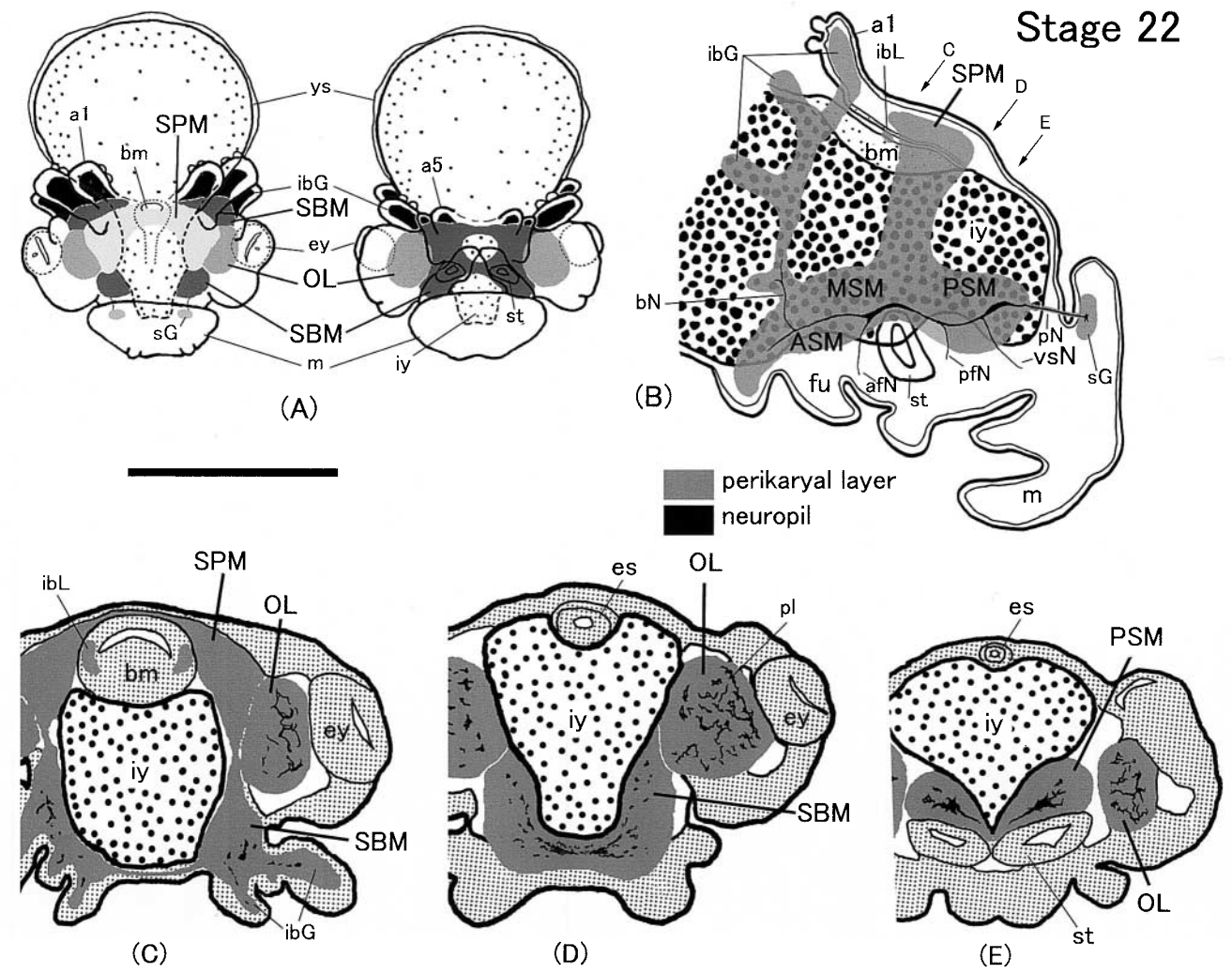

Fig. 4. Developing brain and associated neural elements in the embryo at St 22. (**A**) Dorsal (left) and ventral (right) views of a whole embryo; top anterior. (**B**) Lateral view of the nervous system reconstructed from serial longitudinal sections. The optic lobe is not shown. (**C**)–(**E**) Tracings of transverse sections. Top, dorsal. The approximate position and direction of the sections in **C**–**E** are shown in **B**. a1, arm 1; a5, arm5; afN, anterior funnel nerve; bm, buccal mass; bN, brachial nerve; ey, eye; fu, funnel; ibG, intrabrachial ganglion; ibL, inferior buccal lobe; iy, internal yolk; m, mantle; pfN, posterior funnel nerve; pl, plexiform layer; pN, pallial nerve; sG, stellate ganglion; st, statocyst; vsN, visceral nerve; ys, yolk sac. See Table 1 for other abbreviations. Bar, 0.6 mm for **A** and 0.3 mm for **B**–**E**.

to the OL; no clear boundaries demarcate these compartments. A pair of small masses of neuroblasts, the inferior buccal lobe anlage (ibL), appears on the ventro-lateral surface of the buccal mass (Fig. 4B, C).

From St 22 to St 24, the brain changes conformation from a ring to a solid body with the decrease of the inner yolk (Fig 3A, B, D). The SBM increases in length and thickness with elongation of the head region (Figs. 3C, E, 4B, 5B and 6B). A constriction becomes evident between the ASM and each intrabrachial ganglion (ibG) at St 24 (Fig. 6A, B). The dorsal part of the SPM is still thin at St 23 (Figs. 3B and 5C–E), but markedly increases in thickness at St 24 (Figs.

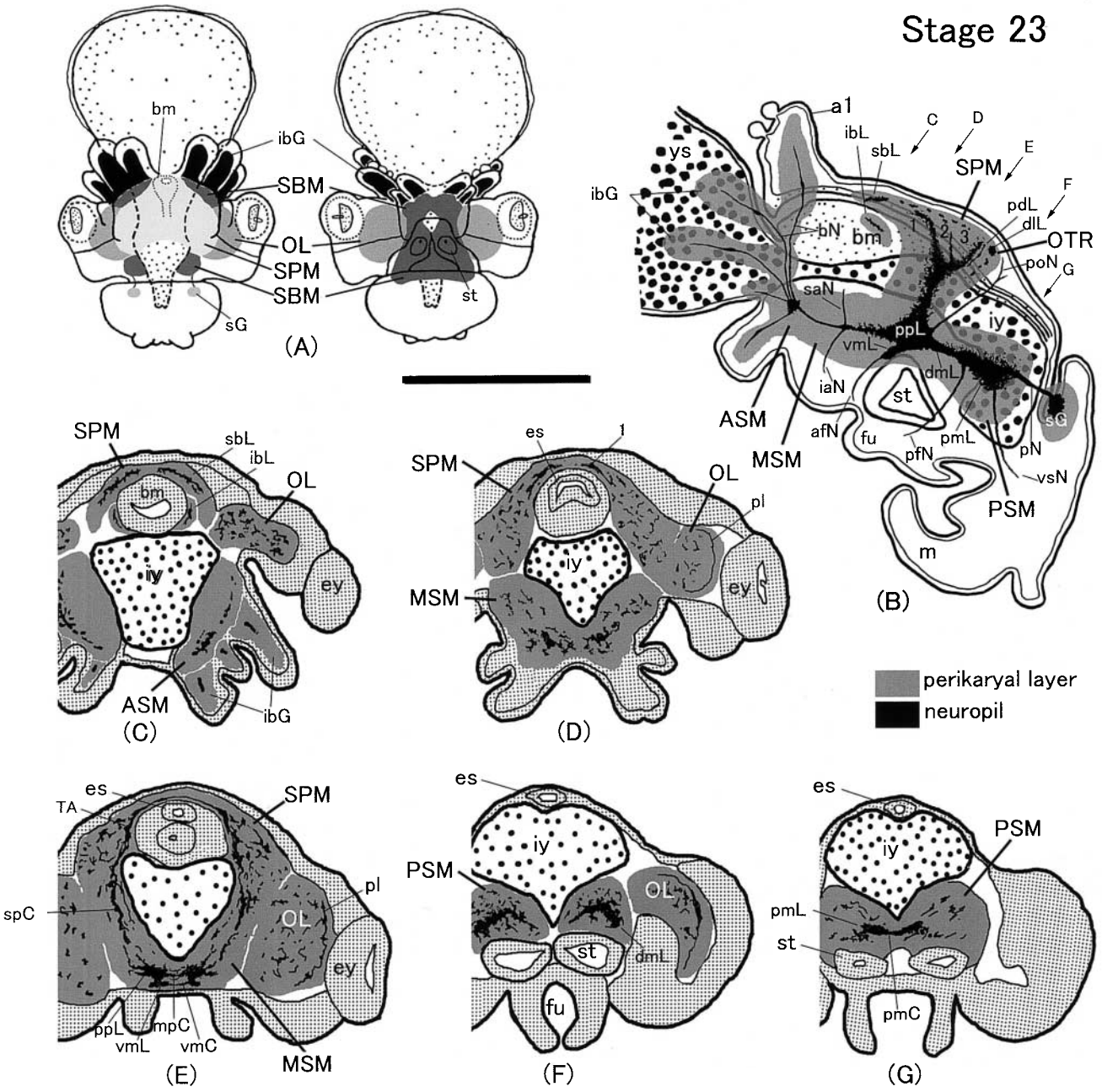

Fig. 5. Developing brain and associated neural elements in the embryo at St 23. (**A**) Dorsal (left) and ventral (right) views of a whole embryo; top, anterior. (**B**) Lateral view of the nervous system reconstructed from serial longitudinal sections. The optic lobe is not shown. Three branches of the transverse arch are shown by 1–3. (**C**)–(**G**) Tracings of transverse sections. Top, dorsal. The approximate position and direction of the sections in **C**–**G** are shown in **B.** a1, arm 1; afN, anterior funnel nerve; bm, buccal mass; bN, brachial nerve; ey, eye; fu, funnel; iaN; inferior antorbital nerve; ibG, intrabrachial ganglion; iy, internal yolk; m, mantle; pfN, posterior funnel nerve; pl, plexiform layer; pmC, posterior magnocellular commissure; pN, pallial nerve; poN, post-orbital nerve; saN, superior antorbital nerve; sG, stellate ganglion; spC, suprapedal commissure; vmC, ventral magnocellular commissure; ys, yolk sac. See Table 1 for other abbreviations. Bar, 0.6 mm for **A** and 0.3 mm for **B**–**G**.

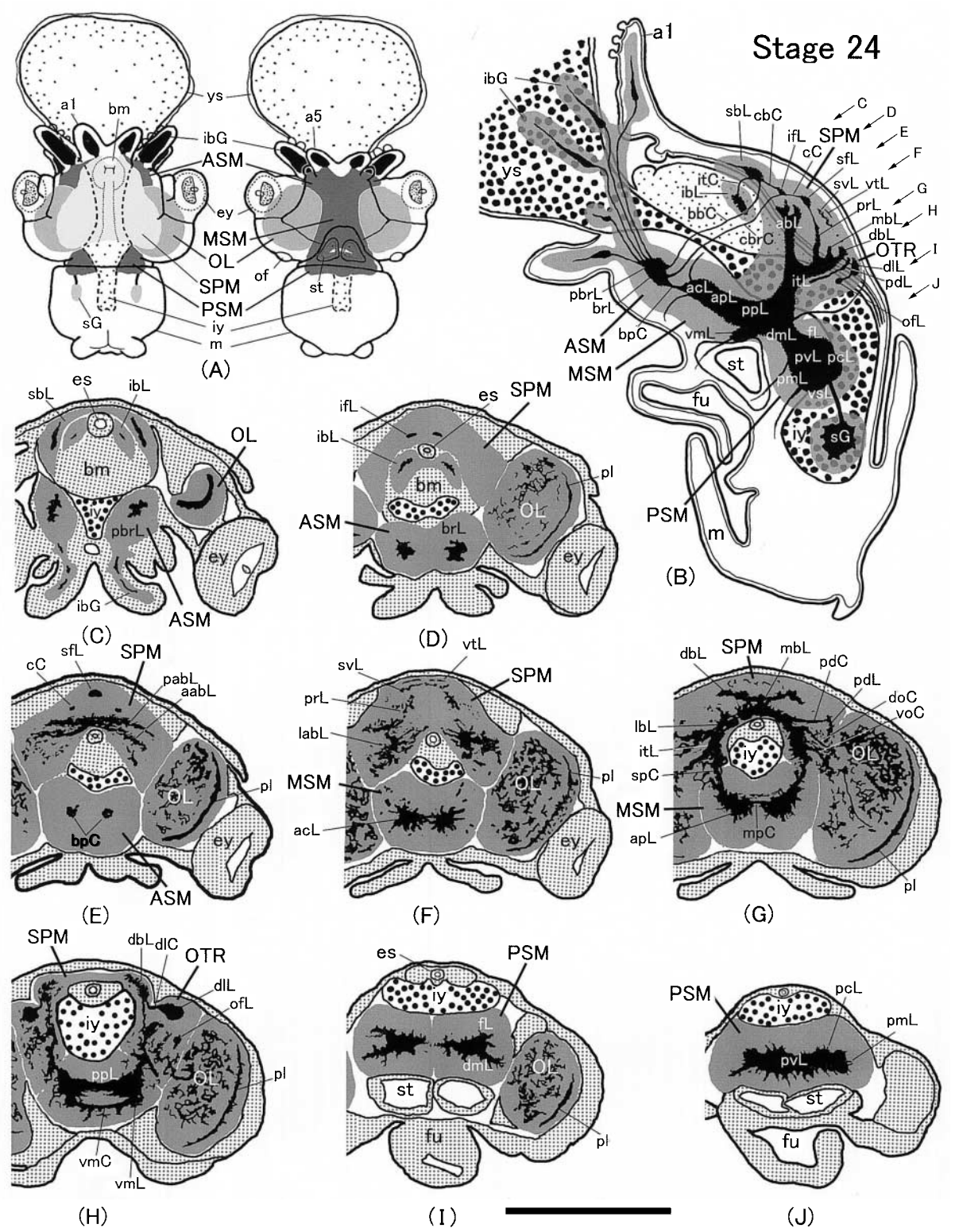

Fig. 6. Developing brain and associated neural elements in the embryo at St 24. (**A**) Dorsal (left) and ventral (right) views of an embryo; top, anterior. (**B**) Lateral view of the nervous system reconstructed from serial longitudinal sections. The optic lobe is not shown. (**C**)–(**J**) Tracings of transverse sections. Top, dorsal. The approximate position and direction of the sections in **C**–**J** are shown in **B**. a1, arm 1; a5, arm 5; bm, buccal mass; bbC, buccal-brachial connective; bpC brachial-pedal connective; cbC, cerebro-buccal connective; cC, cerebral connective; cbrC, cerebro-brachial connective; doC, dorsal route of optic commissure; ey, eye; ibG, intrabrachial ganglion; fu, funnel; itC, interbuccal connective; iy, internal yolk; m, mantle; mpC, middle pedal commissure; of, olfactory organ; sG, stellate ganglion; spC, suprapedal commissure; st, statocyst; vmC, ventral magnocellular commissure; voC, ventral route of optic commissure; ys, yolk sac. See Table 1 for other abbreviations. Bar, 0.6 mm for **A** and 0.3 mm for **B**–**J**.

3D and 6D–G). The SPM protrudes in an anterior direction over the buccal mass at St 23 (Figs. 3C and 5A, B), and a narrow cleft occurs between the protrusion and the main part of the SPM at St 24 (Fig. 3E).

From St 25 to St 27, three structures: the intrabrachial ganglia (ibG), superior buccal lobe (sbL), and anterior subesophageal mass (ASM) are completely separated from the main part of the brain. The intrabrachial ganglia (ibG) are isolated from the ASM at St 25 (Fig. 7A, B). The anterior protrusion of the SPM is isolated from the main part of the SPM at St 25 (Fig. 7A, B). The isolated part of the SPM becomes the superior buccal lobe (sbL) on the postero-dorsal surface of the buccal mass (Figs. 7B). A constriction becomes evident between the ASM and the MSM at St 25, (Fig. 7A, B). They are completely separated from each other at St 27 (cf. Fig. 8A, B).

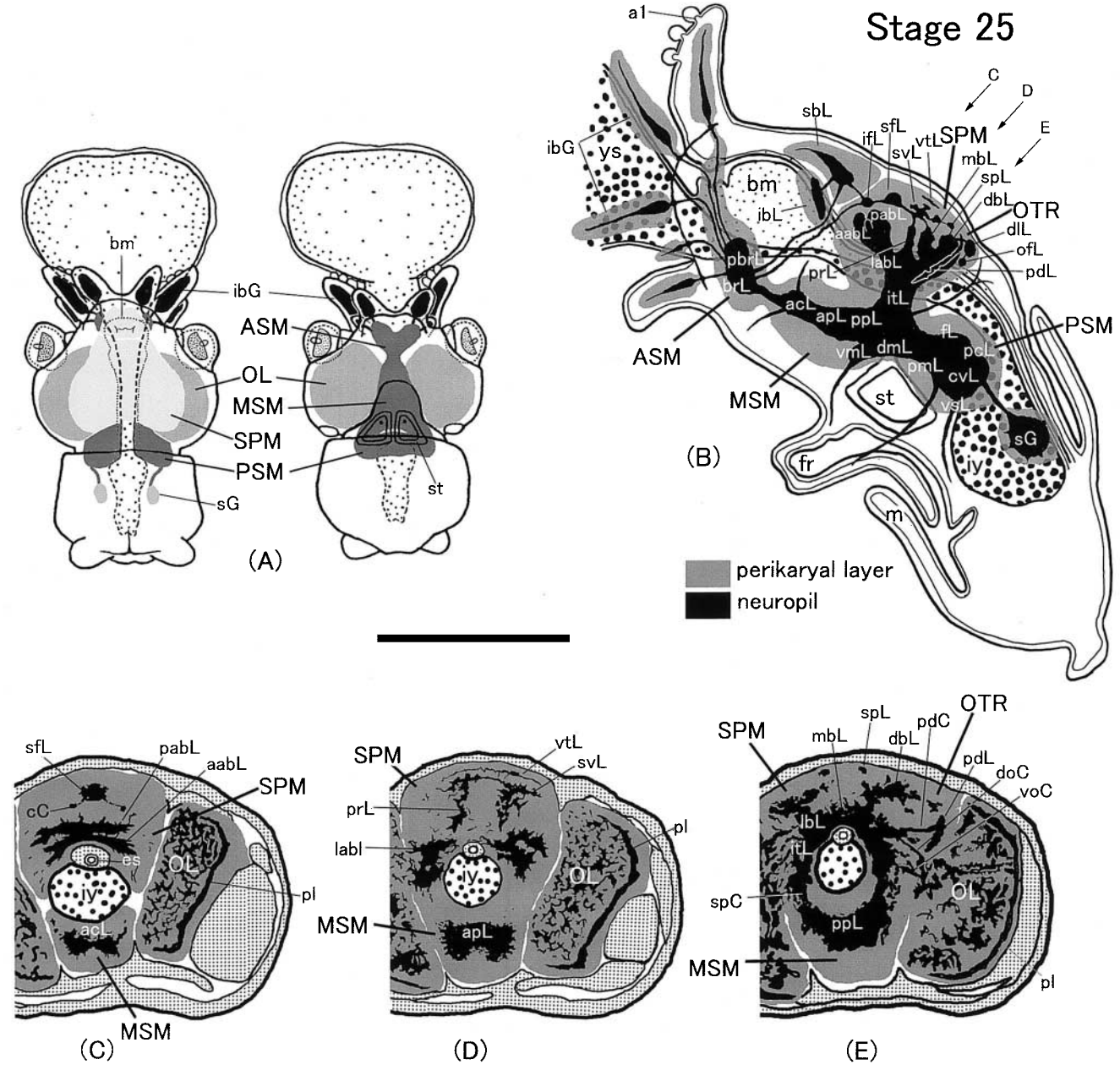

Fig. 7. Developing brain and associated neural elements in the embryo at St 25. (**A**) Dorsal (left) and ventral (right) views of a whole embryo; top, anterior. (**B**) Lateral view of the nervous system reconstructed from serial longitudinal sections. The optic lobe is not shown. (**C**)–(**E**) Tracings of transverse sections. Top, dorsal. The approximate position and direction of the sections in **C**–**E** are shown in **B**. a1, arm 1; bm, buccal mass; bpC brachial-pedal connective; cC, cerebral connective; dlC, dorso-lateral commissure; doC, dorsal route of optic commissure; es, esophagus; ey, eye; ibG, intrabrachial ganglion; fu, funnel; iy, internal yolk; m, mantle; pdC, peduncle commissure; pl, plexiform layer; sG, stellate ganglion; spC, suprapedal commissure; st, statocyst; vmC, ventral magnocellular commissure; voC, ventral route of optic commissure; ys, yolk sac. See Table 1 for other abbreviations. Bar, 0.6 mm for **A** and 0.3 mm for **B**–**E**.

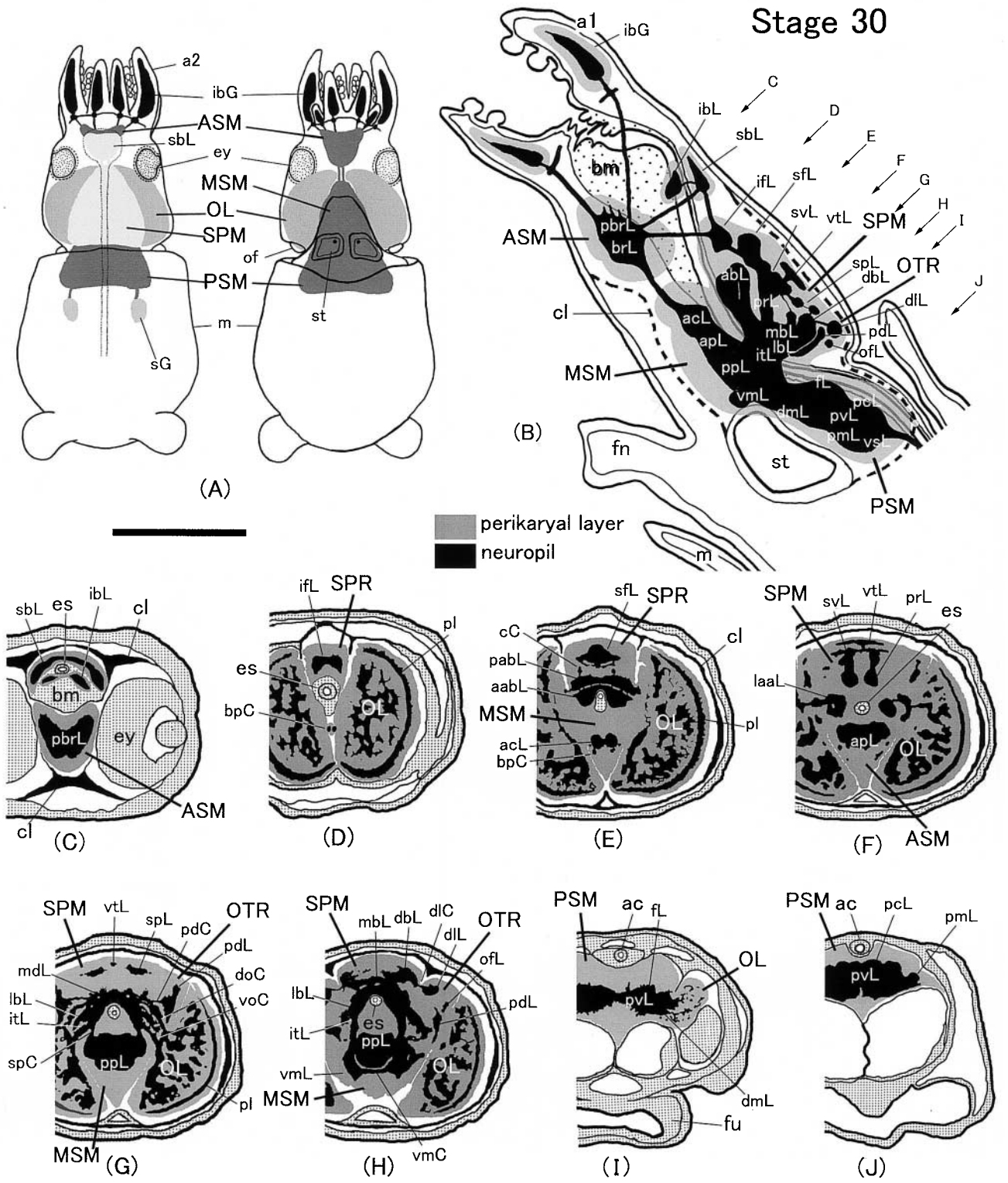

Fig. 8. The developing brain and associated neural elements in the hatchling (St 30). (**A**) Dorsal (left) and ventral (right) views of a hatchling; top anterior. (**B**) Lateral view of the nervous system reconstructed from serial longitudinal sections. The optic lobe is not shown. (**C**)–(**J**) Tracings of transverse sections. The approximate position and direction of the sections in **C**–**J** are shown in **B**. a1, arm 1; a2, arm 2; bm, buccal mass; bpC brachial-pedal connective; cC, cerebral connective; cl, cartilage; dlC, dorso-lateral commissure; doC, dorsal route of optic commissure; ey, eye; fu, funnel; ibG, intrabrachial ganglion; m, mantle; of, olfactory organ; pdC, peduncle commissure; pl, plexiform layer; sG, stellate ganglion; spC, suprapedal commissure; st, statocyst; vmC, ventral magnocellular commissure; voC, ventral route of optic commissure. See Table 1 for other abbreviations. Bar, 0.6 mm for **A** and 0.3 mm for **B**–**J**.

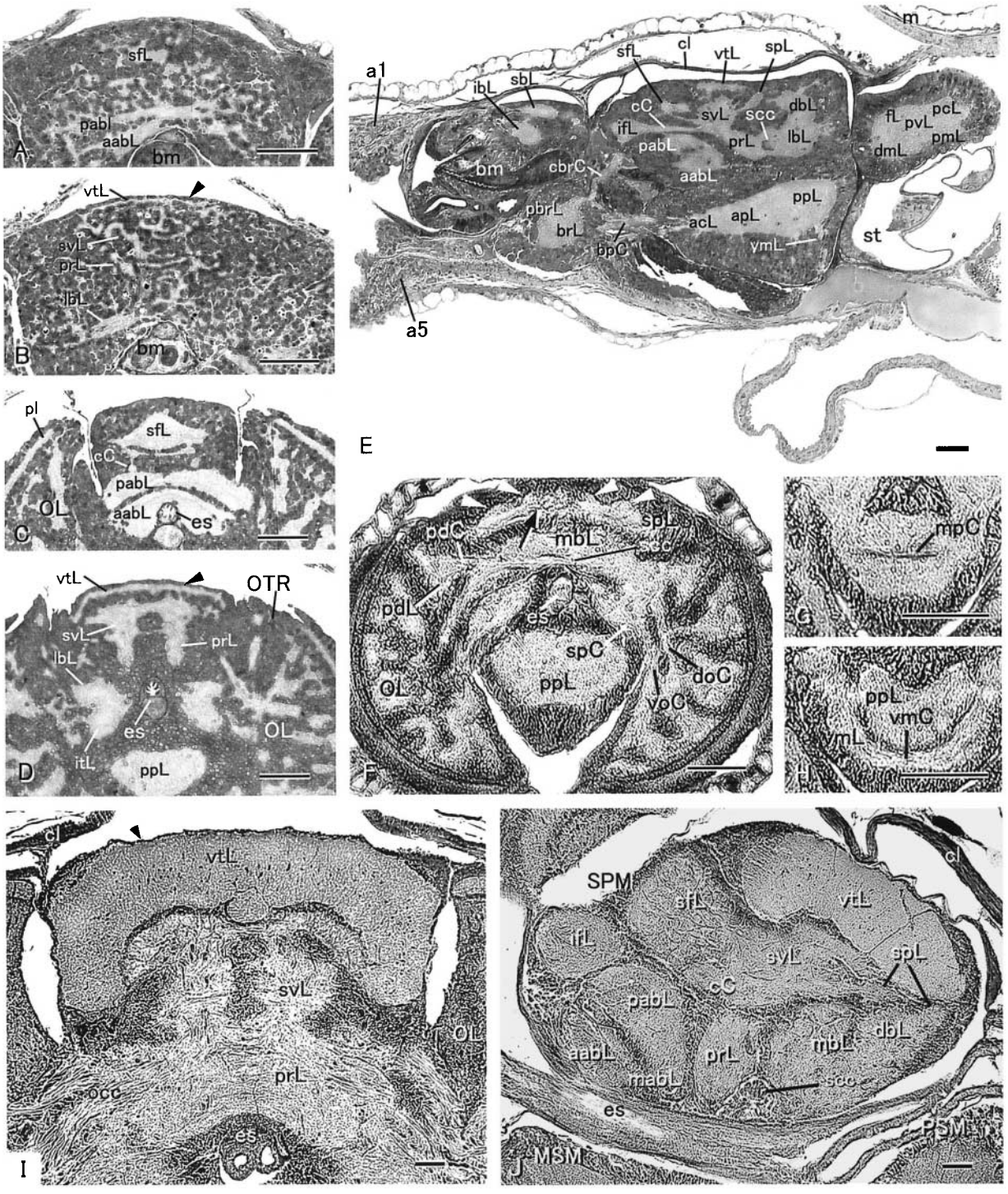

Fig. 9. Light micrographs of the brain in an embryo at St 25, hatchlings, and adults. TB staining (**A**–**E**) and Cajal's silver staining (**F**–**J**). (**A**, **B**) Transverse sections of the supraesophageal mass in the same embryo at St 25. **A** is anterior to **B**. (**C**, **D**) Transverse section of the supraesophageal mass in the same hatchling (St 30). **C** is anterior to **D**. (**E**) Para-sagittal section of the head near the midline in a hatchling. (**F**) Transverse section through a little posterior position to that of **D** in a hatchling. The subpedunculate lobe (spL) shows sub-domains (arrowheads) linked by a commissure (arrow). (**G**, **H**) Transverse sections of the middle subesophageal mass in the same hatchling that in **F**. **G** is anterior to **H**. The middle pedal commissure (mpC) and the ventral magnocellular commissure (vmC) are visible. (**I**) Transverse section of the supraesophageal mass showing the well-developed vertical lobe (vtL) in an adult. (**J**) Longitudinal section of the supraesophageal mass (SPM) in an adult. Arrowheads in **B**, **D**, and **I** indicate the very thin (one cell thick) dorsal perikaryal layer of the vertical lobe (vtL). a1, arm 1; a5, arm 5; bpC, brachial-pedal connective; bm, buccal mass; cbrC, cerebro-brachial connective; cC, cerebral connective; cl, cartilage; doC, dorsal route of optic commissar; es, esophagus; fu, funnel; m, mantle; pdC, peduncle commissure; scc, supraesophageal commissure complex; spC, supra-pedal commissure; st, statocyst; voC, ventral route of optic commissure. See Table 1 for other abbreviations. Bar, 100 μm.

The brain in the hatchling (St 30) (Fig. 8A) is almost identical in conformation to that in the adult (Shigeno and Yamamoto, 2002) except that the dorsal part of the SPM is relatively small. The dorsal part of the SPM markedly increases in relative volume after hatching (cf. Fig. 9E with 9J). The cartilage encapsulating the brain becomes evident at St 30 (Figs. 8B and 9E).

Differentiation of neuropil region

A brain lobe consists of two parts: a central "neuropil region" composed of neurites and an outer "perikaryal layer" occupied by neural and glial cell bodies. The neuropil region is visible as a pale area against the deeply stained perikaryal layer in the TB stained plastic sections. Each brain lobe can be identified on the basis of its position, the characteristic outline of the neuropil region, and the brain nerves arising from the lobe.

Stage 22 (Figs. 3A and 4)

The earliest neuropil is discernible in the subesophageal mass (SBM) and the optic lobe (OL) but no neuropil is detectable in the supraesophageal mass (SPM) by light microscopy. In the cross sections of the SBM, small patches of neuropil are found in the ventral area in the posterior part of the middle subesophageal mass (MSM) (Figs. 3A and 4D) as well as in the posterior subesophageal mass (PSM) (Fig. 4E). Figure 4B — a longitudinal feature reconstructed from serial sections — shows that a thin cord of neuropil runs longitudinally through each side of the SBM (will be referred to as a longitudinal cord). The longitudinal cord is somewhat thick in the posterior region of the MSM and in the PSM. In each optic lobe (OL), small patches of neuropil are scattered in the tangential zone (the major zone of the OL) (Figs. 3A and 4C–E). The plexiform zone (pz) is discernible as a very thin layer of neuropil along the distal surface of the OL facing the base surface of the eye ball (Figs. 3A and 4D).

Some of the major brain nerves are identifiable (Fig. 4B). The posterior end of the longitudinal cord extends out of the brain to the ipsilateral stellate ganglion (sG) as the pallial nerve (pN). The anterior end of the longitudinal cord divides into 5 branches of the brachial nerves (bN), each innervating the intrabrachial ganglion (ibG) within each arm primordium. The longitudinal cord gives off the anterior funnel nerve (afN) from the posterior part of the MSM, and the visceral nerve (vsN) and the posterior funnel nerve (pfN) from the PSM.

Stage 23 (Figs. 3B, C and 5)

The longitudinal cord increases in thickness and becomes a thick column of neuropil from the middle subesophageal mass (MSM) to the posterior subesophageal mass (PSM) but is still thin in the anterior subesophageal mass (ASM) (Fig. 5B–G) (the longitudinal cord will be referred to as the longitudinal column, hereafter). The longitudinal columns lying in both lateral regions of the SBM are connected by three transverse bundles of neuropil (Fig. 5E, G), which correspond to, from anterior to posterior, the median pedal commissure (mpC), ventral magnocellular commissure (vmC), and posterior magnocellular commissure (pmC) described in the adult brain (Shigeno and Yamamoto, 2002). Thus, a pair of the longitudinal columns and three commissural tracts constitute a ladder-like structure, which we have named "the subesophageal ladder" in the embryonic brain of *T. pacificus* (Shigeno *et al*., 2001b).

Brain lobes begin to differentiate along the subesophageal ladder. The posterior pedal lobe anlage (ppL) becomes identifiable in the MSM (Fig. 5B, E). The anterior boundary of the ppL is defined by the middle pedal commissure (mpC). In the posterior part of the MSM, a pair of the ventral magnocellular lobe anlagen (vmL) protrudes a characteristic neuropil region in a ventral direction from the longitudinal columns (Fig. 5B, E). The dorsal magnocellular lobes (dmL) (Fig. 5B, F) and the posterior magnocellular lobe (pmL) (Fig. 5B, G) are differentiating in left and right ventro-lateral margins and the posterior margin of the PSM, respectively. All the main brain nerves have arisen from the SBM, the major ones of which are shown in Fig. 5B.

Within the arched supraesophageal mass (SPM), neuropil also forms an arch (Figs. 3B, C and 5B, E), which we have named "transverse arch" in *T. pacificus* (Shigeno *et al*., 2002b). The bases of the transverse arch continue to the suprapedal commissure (spC) that connects the lateral sides of the posterior pedal lobe (ppL), and the top of the arch crosses the SPM region just over the dorsal surface of the buccal mass (Fig. 5E). Three branches diverge from the transverse arch toward the dorsal zone of the SPM. The branch that elongates in an anterior direction (1 in Figs. 3C and 5B) is forming the neuropil regions of the anterior basal lobes (Table 1). The branch that extends toward the postero-dorsal area of the SPM (3 in Figs. 3C and 5B) is differentiating into the neuropil regions of the posterior basal lobes (Table 1). The thin branch that arises in an anterio-dorsal direction from the base of the posterior branch (2 in Figs. 3C and 5B) is the precursor of the neuropil region of the precommissural lobe. A pair of the neuropil regions of the superior buccal lobe anlage appears in the anteriorly protruding part of the SPM (Fig. 5B, C). No distinct brain lobes but fine neurites are recognizable in the most dorsal zone of the SPM.

In each optic tract region (OTR) — the postero-lateral region of the SPM continuing to the optic lobe (OL) — a small round neuropil region of the dorso-lateral lobe anlage (dlL) and a slender neuropil region of the peduncle lobe anlage (pdL) are identifiable (Fig. 5B). In the OL, plexiform zone (pz) becomes more evident (Fig. 3B).

Stage 24 (Figs. 3D, E and 6)

In the subesophageal mass (SBM), the major brain lobes are all identifiable. The longitudinal columns become thick throughout the SBM except a gap between the anterior subesophageal mass (ASM) and the middle subesophageal

mass (MSM) (Fig. 6B). The neuropil region of two brain lobes, the prebrachial lobe (pbrL) and the brachial lobe (brL), are differentiating (Fig. 6B–D) in the ASM. A pair of neuropil regions of the anterior chromatophore lobe (acL) is identifiable in the anterior end of the MSM. The paired neuropil regions of the brL are connected to those of the acL by a pair of longitudinal tracts, the brachial-pedal connectives (bpC) (Fig. 6B, E). The neuropil region of the anterior pedal lobe (apL) is visible in the middle to the posterior part of the MSM. The boundary between the apL and the posterior pedal lobe (ppL) is defined by the middle pedal commissure (mpC) (Fig. 6G). The ventral magnocellular lobes (vmL), dorsal magnocellular lobes (dmL), and posterior magnocellular lobes (pmL) are evident along the ventro-lateral margin from the MSM to the posterior subesophageal mass (PSM) (Figs. 3E and 6B, H–J). The neuropil region of the palliovisceral lobe (pvL) occupies the greater part of the longitudinal column in the PSM (Figs. 3E and 6B, J). The fin lobes (fL) and the posterior chromatophore lobes (pcL) are identifiable along the dorso-lateral margins of the PSM (Fig. 6B, I, J). The visceral lobe (vsL) is differentiated at the posterior end of the PSM (Fig. 6B).

In the supraesophageal mass (SPM), brain lobes are developing along the three branches, the anterior, middle and posterior branches, diverging from the transverse arch (Figs. 3E and 6B). Along the anterior branch, paired neuropil regions of the anterior anterior basal lobe (aabL), posterior anterior basal lobe (pabL) and lateral basal lobe (labL) are differentiated (Fig. 6E, F). The left and right neuropil regions of the aabL and the pabL meet each other over the esophagus, forming a sub-arch of the transverse arch (Fig. 6E). The posterior branch forms the neuropil region of the dorsal basal lobe (dbL), median basal lobe (mbL), and lateral basal lobe (lbL) (Figs. 3D and 6B, G, H). The neuropil region of the interbasal lobe (itL) is identifiable in the part where the anterior and the posterior branches diverge (Figs. 3E and 6B, G). A pair of neuropil regions of the precommissural lobe (prL) extends in an anterio-dorsal direction from the base of the middle branch (Fig. 6B). A pair of small neuropil regions of inferior frontal lobe (ifL) appears in the antero-dorsal part of the posterior anterior basal lobe (pabL) (Fig. 6B, D). In the dorsal zone of the SPM halfway from the precommissural lobe (prL) to the inferior frontal lobe (ifL), an unpaired neuropil region of the superior frontal lobe (sfL) is identifiable (Fig. 6B, E). Rudimentary neuropil regions of the vertical lobe anlage (vtL) and the subvertical lobe anlage (svL) are discernible in the most dorsal zone of the SPM (Fig. 6B, F).

In addition to the brachial-pedal connectives (bpC) mentioned above, major connectives are all visible in the anterior part of the brain. A pair of tracts, the cerebral connectives (cC), links the neuropil regions of the precommissural lobe (prL) with those of the inferior frontal lobe (ifL) (Fig. 6B, E). A pair of tracts, the cerebro-buccal connectives (cbC), extends from the ifL to the superior buccal lobe (sbL) (Fig. 6B). Connectives are also present between the ifL and the brachial lobe (brL) in the ASM (cerebro-brachial connective, cbrC), between the sbL and brL (buccal-brachial connectives, bbC), and between the sbL and the inferior buccal lobe (ibL) (interbuccal connectives, itC) (Fig. 6B).

In each optic tract region (OTR), the neuropil regions of the peduncle lobe (pdL) and the dorso-lateral lobe (dlL) become larger and more discrete, and a small neuropil region of the olfactory lobe (ofL) is identifiable (Fig. 6B, G, H). In the optic lobe (OL), the plexiform zone (pz) becomes a thick layer of neuropil and many irregular patches of neuropil occupy the tangential zone (Figs. 3D and 6E–H).

Many conspicuous commissural tracts link the left and right OLs or the left and right OTRs through the posterior part of the SPM. These commissural tracts correspond to the peduncle commissure (pdC) (Figs 3D and 6G), dorsolateral commissure (dlC) (Fig. 6H), olfactory commissure, dorsal (doC) and ventral (voC) routes of the optic commissure (Fig. 6G) described in the adult brain (Shigeno and Yamamoto, 2002). The commissural tracts gather into a thick bundle over the esophagus at the position between the median basal lobe (mbL) and the precommissural lobe (prL). We will refer to the commissural bundle as supraesophageal commissure complex (scc).

Stage 25 (Figs. 7 and 9A, B)

The major brain lobes are all identifiable not only in the subesophageal mass (SBM) but in the supraesophageal mass (SPM). Though the brain lobes show an arrangement similar to that in the adult brain, individual lobes are rather immature — the neuropil regions are more or less irregular in outline and cell bodies are not arranged orderly in the perikaryal layers.

In the most dorsal zone of the SPM, the neuropil regions of the accessory lobes (Table 1) are still undeveloped (Fig. 9A, B). The neuropil region of the vertical lobe (vtL) forms a very thin plate expanding underneath the dorsal surface of the SPM (Figs. 7D and 9C). The dorsal perikaryal layer of the vtL is one cell thick, directly exposing to the extra-brain space (Fig. 9B). The neuropil region of the subvertical lobe (svL) is very irregular in outline, facing dorsally the neuropil region of the vtL and continuing ventrally to the paired neuropil regions of the precommissural lobe (prL) (Figs. 7B, E and 9B). Small neuropil regions of the subpedunculate lobe (spL) are discernible in the position posterior to the vtL (Fig. 7B, E). The right and left cerebral connectives (cC) are mutually linked by very thin transverse tracts at the positions of superior frontal lobe (sfL) (Fig. 7C) and the inferior frontal lobe (ifL). Thus, another ladder-like structure which we have named “supraesophageal ladder” (Shigeno *et al*., 2001c) forms in the SPM.

Stage 30 (Figs. 8 and 9C–H)

The arrangement of the brain lobes in the hatchling brain is basically the same as that in the adult brain (Shigeno and Yamamoto, 2002) (Figs. 8B–J and 9E). The neuropil region shows a smooth outline characteristic of

each brain lobe (Fig. 9C, D, E). Cell bodies are orderly arranged in the perikaryal layer of each brain lobe. The proportion of the neuropil region to the perikaryal layer, however, is smaller than that in the adult brain (cf. Fig. 9E with 9J). The accessory lobes (Table 1) in the most dorsal zone of the supraesophageal mass (SPM) are less developed than those in the adult brain (cf. Fig. 9E with 9J). Above all, the vertical lobe (vtL) in the hatchling brain is much smaller than that in the adult brain, though it shows the characteristic feature — the dorsal perikaryal layer is one cell thick and exposed directly to the extra-brain space, and a thin perikaryal layer of a few cells separated the neuropil region from that of the subvertical lobe (svL) (cf. Fig. 9D with I). Enlargement of neuronal cells (neuronal gigantism) as observed in many cephalopod brains (e.g., Shigeno et al., 2001c) is not conspicuous, though neuronal cells are somewhat larger in the SBM than in the SPM.

In the silver-stained sections, well-fasciculated commissures are clearly visible in the SPM (Fig. 9F) and the SBM (Fig. 9G, H). The subpedunculate lobe (spL) shows a characteristic neuropil region consisting of a row of domains linked by a commissural tract (Fig. 9F). Giant axons are not identifiable in the hatchling brain by light microscopy.

DISCUSSION

In the present paper we have described the morphological sequence of the brain development for the first time in the sepioid. It is briefly summarized as follows. The earliest precursors of the brain occur in the form of 4 pairs of neurogenic placodes in the ectoderm undergoing epiboly. In the final stage of epiboly, neuroblasts internalize from the placodes, migrate in between the ectoderm and the mesentoderm, and gather into 4 pairs of ganglionic masses (the cerebral, pedal, palliovisceral, and optic ganglia). The ganglionic masses assemble into a ring encircling the inner yolk and primordial esophagus. During the late embryonic period, the ring gradually transforms into a massive brain, which is composed of 4 domains: a subesophageal mass (SBM), a supraesophageal mass (SPM) and a pair of optic lobes. Before brain lobes begin to differentiate, neuropil forms a simple framework consisting of a longitudinal ladder lying in the SBM (subesophageal ladder), and an arch standing on the lateral sides of the SBM and crossing transversely the SPM (transverse arch). We have clarified using neuron-specific markers that the framework is preceded by a scaffold made of thin axonal bundles (Shigeno et al., in preparation). Differentiation of brain lobes proceeds in a direction from ventral to dorsal along the framework of neuropil; first the magnocellular lobes appear in the SBM, then the basal lobes follow in the proximal part of the SPM, and last the accessory lobes develop in the dorsal-most zone of the SPM.

The embryonic development has been described in many species of the coleoid cephalopod (the cephalopod other than the nautiloid) (Boletzky, 1987). The external patterns of the embryos and their sequential changes closely resemble one another among the species examined so far. Hence, the stages defined by Naef (1928) on the basis of the surface structures of the embryo are widely used as a universal system of staging in cephalopod development (Naef's stages are shown by Roman numerals). Naef (1928), however, has stated that there are heterochronies among internal organ systems.

The spatial pattern of the embryonic brain and its sequential changes revealed in a sepioid, *Idiosepius paradoxus,* were very similar to those previously reported in an octopod, *Octopus vulgaris* (Marquis, 1989), and two teuthoids, *Todarodes pacificus* (Shigeno *et al*., 2001b, c) and *Sepioteuthis lessoniana* (Shigeno *et al*., 2001d). The resemblance of brain development in the 3 major groups of the coleoid cephalopod suggests that the developmental sequence of brain is evolutionally conserved in the coleoid cephalopod. On the other hand, the progression of brain lobe differentiation is differently correlated with the Naef's stage between *T. pacificus* and the other 3 species (*I. paradoxus, S. lessoniana,* and *O. vulgaris*). In *T. pacificus*, the neuropil regions differentiate in St X in the SBM, and from St XVIII to St XX in the SPM (Shigeno *et al.,* 2001c), while in the 3 species, the neuropil regions of all the major brain lobes differentiate during the short period from St XII to St XIV. Thus, in *T. pacificus*, development of brain lobes shows heterochronic retardation in the SPM. *T. pacificus* and *S. lessoniana* belong to the same order, Teuthoidea, and *T. pacificus* and *I. paradoxus* belong to the group that produces the smallest eggs in the cephalopods. Therefore the phylogeny as well as the egg size seems to be irrelevant to the heterochrony. The heterochrony may be related to the mode of post-embryonic life. The hatchlings of the 3 species are predators swimming in search of prey in shallow coastal waters, while the hatchling of *T. pacificus* is presumed to be a suspension feeder, floating passively in offshore waters (O'Dor *et al.,* 1985; Shigeno *et al*., 2001a)

Development of brain lobes must be reflected in the movement and behavior of the embryos and the hatchlings. The brain lobes in the SBM (Table 1) are presumed to be lower and intermediate motor centers controlling individual muscles of the arms, mantle, fins, siphon, eyes and chromatophores (Young, 1976). The anterior and the posterior basal lobes (Table 1) in the SPM are presumed to be the higher motor center, controlling mainly steering and jet propulsion (Young, 1977). The accessory lobes (Table 1) occupying the most dorsal zone of the SPM are presumed to be concerned with the memories and learning for tactile and visual information (Young 1979). The embryos of *I. paradoxus* begin mantle contraction at St 25, and they move the fins, siphon and arms, and often change the position within the egg capsule at St 26 (Yamamoto, 1988). This suggests that lower motor centers in the SBM are functional in St 26. We have found many synapses in the neuropil regions in the SBM and the SPM at St 25 by transmission electron microscopy (unpublished data). We have observed that a hatchling

of *I. paradoxus* swim in an awkward way and catch zoeas of crabs. Since capturing prey requires coordinated movement of the funnel, mantle, and arms, the basal lobes must already be functional in the hatchling. It is not certain whether the very small vertical lobe in the hatchling plays any role in capturing foods. The vertical lobe in the hatchling of *I. paradoxus* was the most immature among hatchlings of 7 coastal species that we have examined: *S. lessoniana* (Shigeno *et al*., 2001a), *Sepia lycidas* and *Octopus ocellatus* (Shigeno *et al*., in preparation), and *Loligo japonica, Loliolus edulis, Sepiella japonica,* and *Eupryma morsei* (unpublished data), but it markedly increased in volume during the post-embryonic period. It has been reported in *O. vulgaris* (Nixon and Mangold, 1996) and *O. ocellatus* (Yamazaki *et al*., 2002) that brain lobes change in relative volume with a change of life style. The marked growth of the vertical lobe seems to be related to a change of life mode. The life mode of *I. paradoxus* changes from planktonic to nekto-benthic during the period of juvenile, and the adults are usually attaching on the back of the eelgrass blades with the dorsal adhering gland. The giant axons in the hatchling of *I. paradoxus* were also too small to be identified by light microscopy. The undeveloped giant axons seem to be correlated with slow and clumsy swimming in the hatchling.

The present paper provides morphological bases for future analyses of brain development in *I. paradoxus*. The following problems are conceivable: (1) How is the two-dimensional pattern of the neurogenic placodes determined in the embryonic surface? Two opposing views have been proposed on the mechanism of the pattern formation of ectodermal placodes: induction by the yolk syncytium (Arnold, 1965; Arnold and Williams-Arnold, 1974) vs. residence of developmental information in the blastodisc (Marthy, 1973, 1975). Analyses of early gene expression will resolve this problem. (2) What is the precise process of the internalization of neuroblasts from the ectodermal placodes? We are now examining neuroblasts undergoing ingression by transmission electron microscopy. (3) How do genes control the three-dimensional arrangement of the brain lobes? We have started isolation of brain-specific genes in *I. paradoxus*. (4) How is the characteristic neuropil region of each brain lobe shaped? We have data suggesting involvement of apoptotic cell death in shaping of the neuropil region (Shigeno *et al*., in preparation). (5) How is morphological elaboration of the brain lobes, particularly the accessory lobes, correlated with behavioral sophistication? The characteristic topology of the vertical lobe seems to facilitate application of electroporation and electrophysiological techniques in the study of functional development of the lobe. We consider that *Idiosepius* is at present the most suitable cephalopod for determining function of genes during development, though many technical difficulties remain to be resolved.

AKNOWLEDGEMENTS

We thank Mr. Waichiro Godo and Dr. Tadashi Akiyama, the Ushimado Marine Laboratory, for their kind help in collecting *Idiosepius paradoxus*.

REFERENCES

Abbott NJ, Williamson R, Maddock L (1995) Cephalopod neurobiology: neuroscience studies in squid, octopus, and cuttlefish. Oxford University Press, Oxford

Arnold JM (1965) The inductive role of the yolk epithelium in the development of the squid *Loligo pealei* (Lesueur). Biol Bull 129: 72–78

Arnold JM, Williams-Arnold LD (1974) Cortical-nuclear interactions in cephalopod development: Cytochalasin B effects on the informational pattern in the cell surface. J Embryol exp Morph 31: 1–25

Boletzky Sv (1987) Embryonic phase. In "Cephalopod life cycles Vol II, Comparative Reviews" Ed by PR Boyle, Acad Press, London, pp 5–60

Budelmann BU (1995) The cephalopod nervous system: What evolution has made of the molluscan design. In "The Nervous System of Invertebrates: An Evolutionary and Comparative Approach" Eds by O Breibach, W Kutsch, Birkhauser, Basel, pp 115–138

Budelmann BU, Young JZ (1993) The oculomotor system of decapod cephalopods: eye muscle, eye muscle nerves, and the oculomotor neurons in the central nervous system. Phil Trans R Soc London B 340: 93–125

Gilbert DL, Adelman WJ, Arnold JM (1990) Squid as experimental animals. Plenum Press, New York.

Kölliker A (1844) Entwicklungsgeschichite der Cephalopoden. Meyer und Zeller, Zürich

Korschlt E (1892) Beiträge zur Entwicklungsgeschichite der Cephalopoden. I. Die Entstehung des Darmkanals und des Nervensystems in Beziehung zur Keimblätterfrage. Verh D Zool Bot Ges Festschr R Leuckart, pp 245–273

Marquis vF (1989) Die Embryonalentwicklung des Nervensystem von *Octopus vulgaris* Lam. (Cephalopoda, Octopoda), eine histologische Analyse. Verh Nat Ges Basel 99 (1): 23–75

Marthy H-J (1973) An experimental study of eye development in the cephalopod *Loligo vulgaris*: determination and regulation during formation of the primary optic vesicle. J Embryol exp Morph 29: 347–361

Marthy H-J (1975) Organogenesis in Cephalopoda: further evidence of blastodisc-bound developmental information J Embryol exp Morph 33: 75–83

Meister G (1972) Organogenese von *Loligo vulgaris* Lam. Zool Jb Anat 89: 247–300

Messenger JB (1979) The nervous system of *Loligo* IV. The peduncle and olfactory lobes. Phil Trans Roy Soc London B 285: 275–309

Naef A (1928) Die Cephalopoden (Embryologie). Fauna Flora Golf Neapel 35 (2): 1–357 [English translation available: Boletzky Sv (2001) The Cephalopoda - Embryology. Smithsonian Institution Libraries, Washington DC]

Nixon M, Mangold K (1996) The early life of *Octopus vulgaris* (Cephalopoda, Octopodidae) in the plankton and at settlement: a change in life style. J Zool Lond 239: 301–327

O'Dor RK, Helm PL, Balch N (1985) Can rhynchoteuthion suspension feed? Vie Milieu 85: 267–271

Sasaki M (1929) A monograph of the dibranchate cephalopods of the Japanese and adjacent waters. J Col Agr Hokkaido Imp Univ 20 (supple 10): 1–357

Shigeno S, Kidokoro H, Goto T, Tsuchiya K, Segawa S (2001a) Early ontogeny of the Japanese common squid *Todarodes pacificus* (Cephalopoda, Ommastrephidae) with special reference to its characteristic morphology and ecological significance. Zool Sci 18: 1011–1026

Shigeno S, Kidokoro H, Tsuchiya K, Segawa S, Yamamoto M (2001b) Development of the brain in the oegopsid squid, *Todarodes pacificus*: An atlas up to the hatching stage. Zool Sci 18: 527–542

Shigeno S, Kidokoro H, Tsuchiya K, Segawa S, Yamamoto M (2001c) Development of the brain in the oegopsid squid, *Todarodes pacificus*: An atlas from hatching to juvenile. Zool Sci 18: 1081–1096

Shigeno S, Tsuchiya K, Segawa S (2001d) Embryonic and paralarval development of the central nervous system of the loliginid squid *Sepioteuthis lessoniana*. J Comp Neurol 437: 449–475

Shigeno S, Yamamoto M (2002) Organization of the nervous system in the pygmy cuttlefish, *Idiosepius paradoxus* Ortmann (Idiosepiidae, Cephalopoda) J Morph 254: 65–80

Stephens PR (1971) Histological methods. In "The anatomy of the nervous system of *Octopus vulgaris*". Ed by JZ Young, Clarendon Press, Oxford, pp 646–649

Yamamoto M (1988) Normal embryonic stages of the pygmy cuttlefish, *Idiosepius pygmaeus paradoxus* Ortmann. Zool Sci 5: 989–998

Yamazaki A, Yoshida M, Uematsu K (2002) Post-hatching development of the brain in *Octopus ocellatus*. Zool Sci 19: 763–771

Young JZ (1965) The central nervous system of *Nautilus*. Phil Trans Roy Soc London B 249: 27–44

Young JZ (1971) The anatomy of the nervous system of *Octopus vulgaris*. Clarendon Press, Oxford

Young JZ (1974) The central nervous system of *Loligo.* I. The optic lobe. Phil Trans Roy Soc London B 267: 263–302

Young JZ (1976) The nervous system of *Loligo.* II. Subesophageal centres. Phil Trans Roy Soc London B 274: 101–167

Young JZ (1977) The nervous system of *Loligo.* III. Higher motor centres. Phil Trans Roy Soc London B 276: 351–398

Young JZ (1979) The nervous system of *Loligo.* V. The vertical lobe complex. Phil Trans Roy Soc London B 285: 311–354

(Received September 9, 2002 / Accepted November 6, 2002)